

# Pair production of charged Higgs bosons at future linear $e^+e^-$ colliders

Marco Battaglia\*

*CERN, Geneva, Switzerland*

Arnaud Ferrari†

*Department of Radiation Sciences, Uppsala University, Sweden*

Ari Kiiskinen‡ and Tuula Mäki§

*Helsinki Institute of Physics, Helsinki, Finland*

(Dated: April 25, 2002 (Rev. Version))

In this paper, the pair production of charged Higgs bosons at possible future  $e^+e^-$  linear colliders is studied. Multi-jet final states are considered and the combinatorial, hadronic and genuine  $t\bar{t}b$  backgrounds are reduced thanks to a kinematical fit. TeV-class and multi-TeV linear colliders are likely to be sensitive to charged Higgs bosons with masses up to  $\simeq 350$  GeV and 1.0 TeV respectively.

## I. INTRODUCTION

The exploration of the origin of mass and of the mechanism of electro-weak symmetry breaking represents one of the main issues on the physics agenda of future colliders. If the Higgs mechanism is indeed responsible for providing matter and force particles with their masses, the detailed exploration of the Higgs sector will most likely require the combination of data from the LHC and lepton colliders. Today there are compelling indications that New Physics is required beyond the Standard Model (SM). In several SM extensions, a second complex scalar Higgs doublet is added yielding five physical Higgs bosons, two of which charged  $H^\pm$ , instead of just one. This is the case in the minimal supersymmetric SM extension (MSSM) and also in non-supersymmetric models (2HDM). The extra Higgs doublet introduces an additional fundamental parameter, describing the ratio of the vacuum-expectation values of the two doublets:  $\tan\beta = v_2/v_1$ .

The negative results of charged Higgs boson searches in the LEP-2 and TEVATRON data and the indirect limits from the rate of the  $b \rightarrow s\gamma$  process have set lower bounds on its mass,  $M_{H^\pm}$ , but the bulk of the parameter space remains still unexplored. At the LHC, charged Higgs bosons can be observed but, according to present studies, only in the limited region of the parameters defined by  $\tan\beta > 10 - 30$ , depending on its mass and detectable decay modes.

In this paper, we discuss the potential of a high energy, high luminosity  $e^+e^-$  linear collider (LC) in the discovery of the charged Higgs boson and in the study of its properties. Since  $M_{H^\pm}$  is not constrained in the models and can vary from the present 78.5 GeV LEP-2 limit [1] up to, and beyond, 1 TeV, different collider energies need to be considered. We concentrate on a TeV-class LC able to deliver  $e^+e^-$  collisions at  $\sqrt{s} = 0.8$  TeV, such as TESLA [2] or an X-band LC [3], and a multi-TeV LC operating at  $\sqrt{s} = 3$  TeV, such as CLIC [4], and discuss the experimental issues specific to the different LC parameters.

Two mass values have been chosen for the charged Higgs boson:  $M_{H^\pm} = 300$  GeV with moderate  $\tan\beta$ , representative of SUSY scenarios with a relatively light Higgs sector, and  $M_{H^\pm} = 880$  GeV with  $\tan\beta = 35$ , as point J from a set of SUSY benchmarks recently proposed [5].

## II. PRODUCTION CROSS SECTION FOR CHARGED HIGGS BOSONS IN $E^+E^-$ COLLISIONS

In  $e^+e^-$  collisions, charged Higgs bosons are pair produced via an intermediate photon or  $Z^0$  boson. At tree level, the production cross section for  $e^+e^- \rightarrow H^+H^-$  only depends on  $M_{H^\pm}$  and on the centre-of-mass energy  $\sqrt{s}$ :

$$\sigma = \frac{e^4}{48\pi s} \left(1 - \frac{4m_H^2}{s}\right)^{3/2} \left(1 + \frac{2c'_V c_V}{1 - m_Z^2/s} + \frac{c'_V{}^2 (c_V^2 + c_A^2)}{(1 - m_Z^2/s)^2}\right)$$

---

\*marco.battaglia@cern.ch

†ferrari@tsl.uu.se

‡ari.kiiskinen@cern.ch

§tuula.maki@cern.ch

However, in calculating the effective cross sections at high energy  $e^+e^-$  collisions, initial state radiation (ISR) and beam-beam effects must be taken into account. Because of the very small transverse dimensions of the beams at the interaction point, the electrons and positrons undergo significant radiation, in the field of the incoming beam, before collision (beamstrahlung). The average energy loss is of the order of 5% for  $\sqrt{s}=0.8$  TeV at TESLA but reaches 31% for  $\sqrt{s}=3$  TeV at CLIC.

When these effects are taken into account, the tree level cross section is folded with the luminosity spectrum. For the low values of  $M_{H^\pm}$  the effective cross section is enhanced compared to the tree level cross section, while close to the kinematical threshold only a smaller fraction of the energy spectrum is available and the effective cross section is reduced as exemplified in Figure 1. Corrections to the  $H^+H^-$  production cross section have been computed at one loop and found to become sizeable in some region of the parameter space [6]. A precise determination of the cross section can thus provide additional information on model parameters.

When considering only decays to SM particles, the dominant  $H^-$  decay modes are those involving the heaviest quark or lepton pairs accessible, i.e.  $t\bar{b}$  and  $\tau^-\bar{\nu}_\tau$ [10], as shown in Figure 2 for two values of  $\tan\beta$ . The dependence of the dominant branching fractions on  $\tan\beta$  can be exploited for determining this fundamental parameter of the theory. In this study we consider the fully hadronic  $e^+e^- \rightarrow H^+H^- \rightarrow (t\bar{b})(\bar{t}b)$  channel, which leads to two  $W$  bosons and four  $b$  quarks in the final state and provides with a direct reconstruction of  $M_{H^\pm}$ .

### III. EVENT RECONSTRUCTION

The SIMDET parametrised detector simulation [7] has been used to account for the anticipated experimental resolutions of a LC detector. The  $b$ -tagging performance, which is of major importance in this analysis, has been included, assuming an efficiency  $\epsilon_b = 0.90$ . The characteristic signal final state, including four  $b$  jets and the intermediate  $W$  and  $t$  mass constraints, guarantees an efficient rejection of most multi-fermion background processes. The cross section of the irreducible  $t\bar{b}t\bar{b}$  background has been estimated using the COMPHEP program [8] at 0.8 TeV and 3 TeV and found to be 5.5 fb and 1.5 fb respectively.

Hadronic jets have been reconstructed using the CAMJET clustering algorithm, for the 0.8 TeV analysis, and the Lund algorithm for 3 TeV, tuning the cut-off to maximise the number of eight jet events for the signal. In order to distinguish the production of charged Higgs bosons from the associated background processes and to accurately measure its mass, it is important to obtain a clean mass distribution of the multi-jet final states. Therefore only hadronic  $W$  boson decays have been considered by removing events with significant transverse missing energy or tagged leptons.

The mass reconstruction has been performed as follows. In a first step, the presence of two  $W$  bosons decaying hadronically has been tested. The assignment of the four non- $b$  tagged jets to their correct  $WW$  pair has been done by choosing the combination which minimises the difference between the di-jet masses and the  $W$  mass. In a second step, each  $t$  quark has been reconstructed from a  $W$  candidate paired with one of the four  $b$  tagged jets, taking the combination giving the invariant mass closest to the top mass. Each of the charged Higgs bosons has then been reconstructed from a  $t$  candidate paired with one of the two remaining  $b$  tagged jets and selecting the configuration minimising the mass difference of the two  $t\bar{b}$  pairs. Events with no jet combination compatible with the  $W$  or  $t$  masses within the observed resolution have been discarded. An event kinematical fit has been finally applied to improve the mass resolution. The fit uses energy and momentum conservation, the  $W$  and  $t$  mass constraints and imposes  $H$  boson equal mass.

#### A. $M_H = 300$ GeV at a TeV-class LC

At  $\sqrt{s} = 0.8$  TeV, the reconstructed mass peak has a width of 6.2 GeV with a natural  $H^\pm$  width of 4.3 GeV, for  $M_{H^\pm} = 300$  GeV. This corresponds to a mass resolution of 1.5%. The signal reconstruction efficiency has been found to be 0.022, corresponding to 149 signal with 24 background events, in a signal mass window of  $\pm 2.5\sigma$  around the mass peak. The good mass resolution achieved with the kinematical fit gives a signal significance  $S/\sqrt{B}=30$  (see Figure 3). The product  $\sigma(e^+e^- \rightarrow H^+H^-) \times \text{BR}(H^- \rightarrow t\bar{b})$  can be measured to an accuracy of 8.8%.

The maximum reach in mass for a 5  $\sigma$  discovery has been studied by analysing signal samples generated at different Higgs mass. The largest observable Higgs mass corresponds to about 350 GeV, corresponding to the detection of 47 signal events, with the same number from background for 1  $\text{ab}^{-1}$  of data at  $\sqrt{s} = 0.8$  TeV.

At moderate  $\tan\beta$  values, as well as in scenarios where the couplings to fermions are suppressed, the  $H^- \rightarrow W^-h^0$  decay, leading to the same  $W^-b\bar{b}$  decay final state, may become sizeable. In order to study this process, a similar mass reconstruction procedure can be applied except for the top quark constraint being replaced by

the  $h^0$  one. By comparing the  $\chi^2$  of the fit for the two hypotheses, the  $H^- \rightarrow \bar{t}b$  and  $H^- \rightarrow W^- h^0$  decays can be efficiently distinguished.

### B. $M_H = 880$ GeV at a multi-TeV LC

At a multi-TeV collider the decay reconstruction is complicated by the larger beamstrahlung, as mentioned above, and by the  $\gamma\gamma \rightarrow$  hadrons background [9] overlayed to each  $e^+e^-$  collision.

The reconstruction procedure for the charged Higgs boson follows closely that described above, but special care has been taken to make the result robust in presence of the  $\gamma\gamma$  background, while the broader luminosity spectrum affects the kinematic fit, as discussed below. The additional hadrons generated by these  $\gamma\gamma$  collisions, mostly affecting the forward regions, may either be merged into the jets coming from the  $H^\pm$  decay or result in extra jets being reconstructed. It is therefore important to minimise the impact from this background source on the event reconstruction. In this analysis only the four leading non- $b$  jets have been considered, together with the  $b$ -tagged jets. In addition the resulting invariant masses of the intermediate states are biased towards higher values due to the additional hadron contribution. This needs to be taken into account by calibrating the mass response with simulation including the  $\gamma\gamma$  background.

Due to the significant loss of energy of the colliding  $e^+$  and  $e^-$ , energy and momentum conservation constraints cannot be applied on the reconstructed system for the nominal  $\sqrt{s}$ . Instead the kinematical fit allows for an extra particle to be radiated but imposes its transverse momentum to be zero. The kinematic fit allows to improve, by a factor of two, the resolution on the mass reconstruction for  $H$  candidates. Furthermore, the use of the kinematical fit, allows to correct for the effect of the  $\gamma\gamma$  background resulting in a mass peak of the charged Higgs boson at the position of the generated mass (see Figure 4).

The signal event rate has been estimated for  $M_H = 880$  GeV, first disentangling the  $\gamma\gamma$  background and then assuming that the detector integrates the background from 15 bunch crossings (BX). In the first case with an integrated luminosity is  $3 \text{ ab}^{-1}$  and assuming  $\text{BR}(H \rightarrow tb) = 1.0$ , the r.m.s. of the mass peak, after the kinematical fit, is 33 GeV with a  $H^\pm$  natural width of 21 GeV. 47  $e^+e^- \rightarrow H^+H^- \rightarrow (\bar{t}b)(\bar{t}b)$  signal events are expected to be reconstructed within the  $\pm 2.5\sigma$  signal mass region, corresponding to a signal efficiency of  $\simeq 0.02$ .

When the hadronic background, integrated over 15 BX is included, the peaks of the intermediate  $W$  and  $t$  states are shifted towards higher masses and get significantly wider. To account for this effect, the mass windows for the reconstructed  $W$  boson and  $t$  quark need to be shifted and made 50% wider. The fitted signal width becomes 42 GeV and there are 51  $e^+e^- \rightarrow H^+H^- \rightarrow (\bar{t}b)(\bar{t}b)$  signal events with a reconstructed mass in the signal window, corresponding to an efficiency comparable to the previous case. The  $t\bar{t}b$  background processes contribute 24 events for  $3 \text{ ab}^{-1}$ . By scaling these results, the estimated maximum mass reach for a  $5\sigma$  discovery with  $3 \text{ ab}^{-1}$  at 3 TeV is  $\simeq 1.0$  TeV.

Beyond discovery the properties of the charged Higgs boson needs to be studied. These include the mass, the production rate and the decay branching fractions. The mass can be measured to an accuracy of 1% for 15 integrated BX and the product  $\sigma(e^+e^- \rightarrow H^+H^-) \times \text{BR}(H^- \rightarrow \bar{t}b)$  can be measured to an accuracy of  $\simeq 20\%$ .

## IV. CONCLUSIONS

The full reconstruction of the charged Higgs boson  $H^+H^- \rightarrow \bar{t}b\bar{t}b$  multi-jet final states has been studied for two scenarios:  $M_{H^\pm} = 300$  GeV at  $\sqrt{s} = 800$  GeV and  $M_{H^\pm} = 880$  GeV with  $\sqrt{s} = 3$  TeV. The analyses are based on the reconstruction of hadronic events with eight jets, four of which  $b$ -tagged. A kinematical fit taking into account the  $W$  and  $t$  intermediate mass constraints and energy-momentum conservation has been applied to reject the multi-fermion background and optimise the mass resolution for signal events. The Higgs mass can be reconstructed with an accuracy of  $\simeq 1\%$  and the product  $\sigma(e^+e^- \rightarrow H^+H^-) \times \text{BR}(H^- \rightarrow \bar{t}b)$  can be measured to an accuracy of 8.8% for  $M_{H^\pm} = 300$  GeV at 0.8 TeV and 15% for  $M_{H^\pm} = 880$  GeV at 3 TeV.

For further studies, a more efficient event selection needs to be envisaged. An interesting possibility is to tag the  $e^+e^- \rightarrow H^+H^-$  event by reconstructing only one  $H \rightarrow tb$  decay. This allows to increase the event selection efficiency and to study the  $H$  decay in the hemisphere opposite to the tagged one in an unbiased way.

## ACKNOWLEDGMENTS

We are grateful to E. Boos for his help with the COMPHEP package.

The research activity of A.F. has been supported by a Marie Curie Fellowship of the European Community programme *Improving Human Research Potential and the Socio-economic Knowledge Base* under contract number HPMF-CT-2000-00865.

#### REFERENCES

- [1] LEP Higgs WG, *Search for charged Higgs bosons: preliminary combined results using LEP data collected at energies up to 209 GeV*, contributed paper to the XXXVIth Rencontres de Moriond, Les Arcs, France, 10-17 March 2001, LHWG internal note 2001-1.
- [2] *The Superconducting Electron-Positron Linear Collider with an Integrated X-Ray Laser Laboratory Technical Design Report*, DESY 2001-011.
- [3] *2001 Report on the Next Linear Collider*, SLAC-R-571.
- [4] The CLIC Study Team, *A 3 TeV  $e^+e^-$  linear collider based on CLIC technology*, CERN 2000-008.
- [5] M. Battaglia *et al.*, *Proposed Post-LEP Benchmarks for Supersymmetry*, to appear on *E. Phys. J. C* and hep-ph/0106204.
- [6] J. Guasch, W. Hollik and A. Kraft, *Nucl. Phys. B* 596 (2001), 66.
- [7] M. Pohl and H.J. Schreiber, "SIMDET - A parametric Monte Carlo for a TESLA detector", DESY 99-030.
- [8] A. Pukhov *et al.* *CompHEP - a package for evaluation of Feynman diagrams and integration over multi-particle phase space*, hep-ph/9908288.
- [9] D. Schulte, *Background at future linear colliders*, CERN-PS-99-066.
- [10] In the following the notation of a particle implies also its anti-particle

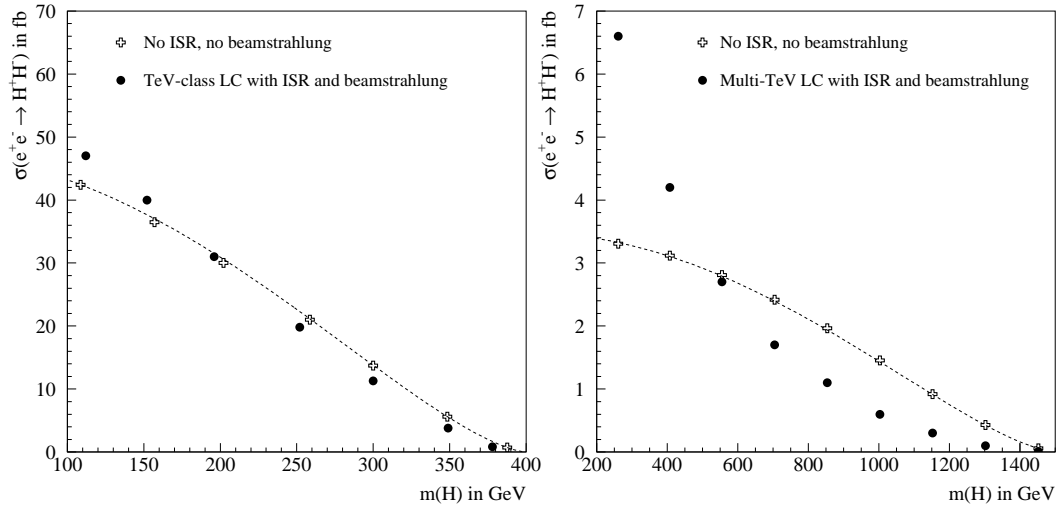


FIG. 1: Cross section for  $e^+e^- \rightarrow H^+H^-$  at  $\sqrt{s} = 800$  GeV (left) and at  $\sqrt{s} = 3$  TeV (right). Open crosses and dashed lines show the cross section at tree level, while full circles show the effective cross section after including ISR and beamstrahlung.

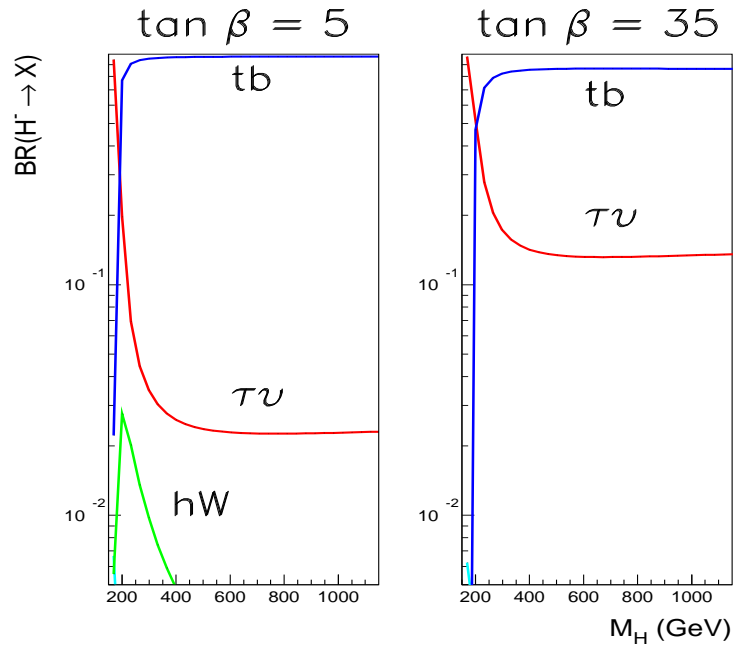


FIG. 2:  $H^\pm$  branching fractions for the dominant decay modes as a function of  $M_{H^\pm}$  for two values of  $\tan \beta$ .

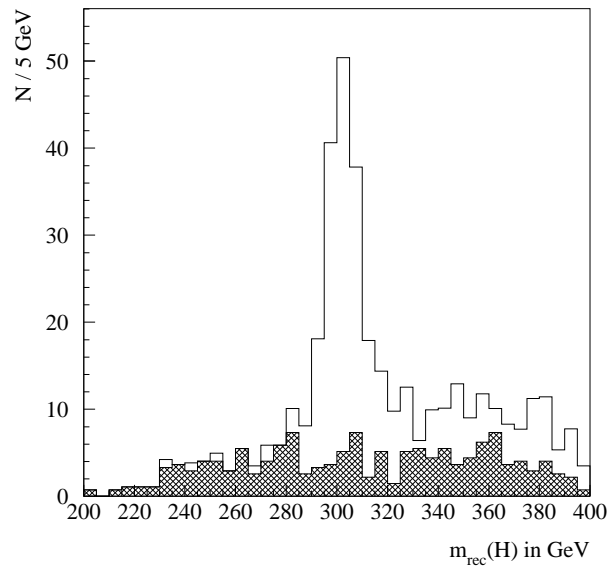


FIG. 3: Fitted charged Higgs boson mass for  $H^+H^- \rightarrow (t\bar{b})(\bar{t}b)$  with  $m_H = 300$  GeV. The histogram is normalised to an integrated luminosity of  $1 \text{ ab}^{-1}$ , with a 100% branching ratio in the analysed decay mode. The contribution of the  $t\bar{t}b$  background events is shown by the dark histograms.

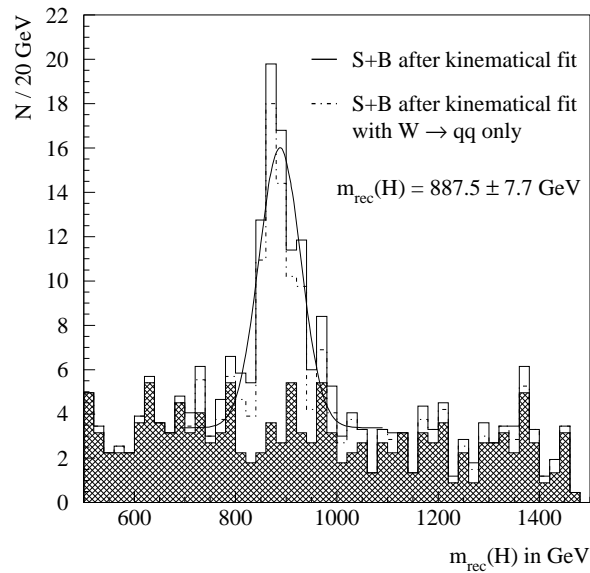


FIG. 4: Reconstructed  $H^\pm \rightarrow tb$  invariant mass after the kinematical fit for an integrated luminosity of  $3 \text{ ab}^{-1}$ . The  $t\bar{t}b$  background is shown by the hatched distribution.